JABFM
eISSN 2280-8000

J Appl Biomater Funct Mater 2017; 15(2): e176-e183
DOI: 10.5301/jabfm.5000340

ORIGINAL RESEARCH ARTICLE

Open Access

Titanium-hydroxyapatite composites sintered at low temperature for tissue engineering: in vitro cell support and biocompatibility

Romina Comín[1], Mariana P. Cid[1], Luciano Grinschpun[2], Carlos Oldani[2], Nancy A. Salvatierra[1]

[1] IIBYT-UNC-CONICET, Department of Chemistry, School of Exact, Physics and Natural Sciences, National University of Córdoba, Córdoba - Argentina
[2] Department of Materials, School of Exact, Physics and Natural Sciences, National University of Córdoba, Córdoba - Argentina

ABSTRACT

Background: In clinical orthopedics, a critical problem is the bone tissue loss produced by a disease or injury. The use of composites from titanium and hydroxyapatite for biomedical applications has increased due to the resulting advantageous combination of hydroxyapatite bioactivity and favorable mechanical properties of titanium. Powder metallurgy is a simple and lower-cost method that uses powder from titanium and hydroxyapatite to obtain composites having hydroxyapatite phases in a metallic matrix. However, this method has certain limitations arising from thermal decomposition of hydroxyapatite in the titanium-hydroxyapatite system above 800°C. We obtained a composite from titanium and bovine hydroxyapatite powders sintered at 800°C and evaluated its bioactivity and cytocompatibility according to the ISO 10993 standard.
Methods: Surface analysis and bioactivity of the composite was evaluated by X-ray diffraction and SEM. MTT assay was carried out to assess cytotoxicity on Vero and NIH3T3 cells. Cell morphology and cell adhesion on the composite surface were analyzed using fluorescence and SEM.
Results: We obtained a porous composite with hydroxyapatite particles well integrated in titanium matrix which presented excellent bioactivity. Our data did not reveal any toxicity of titanium-hydroxyapatite composite on Vero or NIH3T3 cells. Moreover, extracts from composite did not affect cell morphology or density. Finally, NIH3T3 cells were capable of adhering to and proliferating on the composite surface.
Conclusions: The composite obtained displayed promising biomedical applications through the simple method of powder metallurgy. Additionally, these findings provide an in vitro proof for adequate biocompatibility of titanium-hydroxyapatite composite sintered at 800°C.

Keywords: Biocompatibility, Composite, Hydroxyapatite, Powder metallurgy, Titanium

Introduction

In clinical orthopedics, a critical problem is the bone tissue loss produced by a disease or injury. Hydroxyapatite ($Ca_{10}(PO_4)_6(OH)_2$) (HA) is a bioceramic material frequently used for implants of human hard tissue because its chemical and crystallographic structure is similar to that of bone minerals of mammalian bones and teeth (1-3). As a result, HA is nontoxic, bioactive and biocompatible (4) allowing osseointegration between implants and bones (5). HA can be obtained from animal bones, or it can be artificially produced. However, in clinical applications, the use of synthetic HA has several disadvantages, such as its higher dissolution rate in physiological environments, which can trigger an immune response (6-9), and the high cost of the raw materials. Therefore, natural HA is more suitable to biomedical applications (10). A major limitation of using HA is its poor mechanical properties (11, 12). In contrast, although titanium (Ti) is a biocompatible metal with better mechanical properties, its biocompatibility is not as good as that of HA. Moreover, failure of the implantation can be observed due to poor interaction between the host bone and titanium, which can result in loss of the implant (13). Consequently, with the purpose of generating high efficiency biomaterials for bone replacements, Ti-HA composites have been considered an encouraging group of materials for research and development of implants. Different methods of HA coatings on Ti surfaces have been tested (14-20). It has been reported that in implants coated with HA, it facilitates attachment to the bone surface, leading to a higher integration

Accepted: December 21, 2016
Published online: February 21, 2017

Corresponding author:
Dr. Nancy A. Salvatierra
Departamento de Química
Facultad de Ciencias Exactas Físicas y Naturales
Universidad Nacional de Córdoba
Av. Vélez Sarsfield 1611
5016 Córdoba, Argentina
nancy.salvatierra@unc.edu.ar

rate compared with uncoated implants in in vitro and in vivo experiments (21, 22). However, HA coating stabilization can only be observed for a short time, since bone formation, integration and stability around implants (coated and uncoated ones) does not show any differences at 6 months after implantation.

Another method to get Ti-HA composites is powder metallurgy (PM) (23-25). PM uses powders from Ti and HA to obtain sintered composites with HA particles as "islands" in the Ti matrix. This method simplifies and reduces the cost of the composite by using TiH_2 powder instead of pure Ti. Additionally, the sintering at the final stage of the process allows control of the surface porosity. Although pure HA is stable in an inert argon atmosphere at temperatures as high as 1200°C (26), it has been reported that in a Ti-HA system, the dehydroxylation and decomposition of HA was accelerated by the presence of Ti to form tetracalcium phosphate and calcium oxide at temperatures above 800°C (27). This imposes certain limitations on the thermal conditions that can be used for the manufacture of Ti-HA composites. Another important issue to consider is the amount of HA in the composite, Popa et al (28) reported that the "amount of HA is of major importance and has to be kept within strict limits: too much (more than 30%) leads to excessive brittleness, whereas too little (5%) in contact with the bone is insufficient for the required bioactivity."

Lastly, the innovation of new biomaterials requires methodical and quantitative assessment of the biocompatibility of their components (29). In fact, biomaterial biocompatibility is very intimately related to cell behavior in contact with the material, particularly to the adhesion to its surface.

In the present study, we sintered a composite of Ti and bovine HA at 800°C in an argon atmosphere and evaluated its bioactivity and cytocompatibility according to the ISO 10993 standard for composite extracts. Furthermore, we assessed proliferation and adhesion of Vero and NIH3T3 cells on the composite surface.

Materials and methods

Preparation of composites

Ti-HA composites were prepared by PM from TiH_2 98% pure (Sigma) mesh-325 and bovine HA (Inbiomed S.A., Argentina). TiH_2 powder was mixed 20% HA powder (Ti-20HA), and the mixture was homogenized for 30 minutes. The powders were compacted at 390 MPa without addition of lubricant to obtain samples of size 8-mm diameter and 2-mm height. Then, these were sintered in an argon atmosphere at atmospheric pressure at 800°C for 2 hours. This inert atmosphere is achieved with argon preflow for 30 minutes. Hydrogen from TiH_2 was released at the beginning of the sintering step by heating samples at 500°C for 30 minutes. Discs of pure Ti (Ti) and porous Ti (Ti-Por) were prepared in the same way, with Ti-Por being obtained from a mixture of Ti with 20% in NH_4HCO_3. All composites were ultrasonically cleaned in 100% acetone, then with distilled water for 10 minutes at each step, and then were sterilized by dry heat at 140°C for 2 hours.

Surface characterization and in vitro bioactivity of Ti-HA composites

To investigate the chemical and structural composition of the samples, X-ray diffraction (XRD) analyses in a Philips PW1800/10 diffractometer (LAMARX-UNC) were carried out. The surface topography of composites was examined by scanning electron microscopy (SEM) using a FE-SEM ΣIGMA microscope at 12 kV (LAMARX-UNC). The samples were mounted on stubs and sputtered coated with chrome. To analyze their bioactivity, Ti-HA composites were immersed in simulated body fluid (SBF) (30) and kept at 37°C. After 5 and 10 days, surface composites were examined by SEM.

Preparation of composite extracts

Extracts of all composites were prepared to assess the hazard potential of samples. Extraction conditions were selected in accordance with ISO 10993-12 (31). The sterilized composites were put into sterile, chemically inert and closed containers. Dulbecco`s modified Eagle's medium (DMEM) (Gibco) was added at a ratio of 0.1 g/mL (mass of disc to volume of DMEM). Then, samples were incubated in a humidified atmosphere of 5% CO_2 in air at 37°C for 72 hours. The discs were removed from the media, and a 100% extract (100-extract) was obtained after addition of fetal bovine serum (FBS) (PAA) (10% v/v). For the cytotoxicity assay, 75%, 50% and 25% extracts (75-, 50-, 25-extracts) were obtained by dilution in supplemented DMEM of 100-extract.

Cell culture

Experiments were performed using the epithelial Vero cell line and fibroblastic NIH3T3 cells (provided by CIQUIBIC-Argentina).The Vero cell line is mandatory for cell cytotoxicity and cell–substratum interaction studies in biomaterial research (32). In addition, the NIH3T3 cells were also used here because they share a common origin with osteoblastic cells. Both cell lines were cultured in DMEM with 10% FBS, 4 mM of L-glutamine (Gibco), 4 mM of sodium pyruvate (Sigma) and 10,000 IU/mL of penicillin with 10,000 µg/mL of streptomycin in a humidified 5% CO_2 atmosphere at 37°C. Cells were seeded on 96-well plates at a density of 10,000 cells per well and incubated in supplemented DMEM. The culture medium was replaced every 3 days.

Cytotoxicity assay

Cytotoxicity of extract composites was performed by the MTT assay (33), according to ISO 10993-5 (32). Vero or NIH3T3 cells were seeded as described above for 24 hours, after which media were removed, and extracts from different composites were added. After 24 hours, cells were rinsed with phosphate-buffered saline (PBS) twice, and 50 µL of 1 mg/mL MTT in DMEM was added to the appropriate wells and incubated at 37°C for 1.5 hours. The formazan crystals formed were dissolved by adding isopropyl alcohol in each well. Absorbance was quantified at 595 nm using a Multiskan Spectrum microplate reader (Thermo Scientific). High-density polyethylene (HDPE) 100-extract (ratio of 6 cm^2/mL, surface of HDPE to volume of DMEM) was used as negative

control, and 0.2% phenol solution was assayed as positive control. The percentage of cell viability was calculated according to the optical density measured for each incubation condition with respect to the optical density determined for cells grown in supplemented DMEM ×100. All experiments were carried out in sextuplicate.

Cell morphological analysis

The morphology of Vero and NIH3T3 cells grown in the presence of extracts of composite was observed by microscopy (34). The morphology and relative density of Vero cells cultured in the presence of 100-extract or supplemented DMEM were examined using SEM (JEOL JSM 6480 Brand LV; Iniqui, Argentina). Cells were plated at a density of 10,000 cells/cm^2 on glass coverslips, and incubated in the presence of 100-extracts or supplemented DMEM for 4 days. After incubation, samples were washed with PBS and fixed overnight in 4% glutaraldehyde buffered in PBS at 4°C. Next, the samples were washed 3 times with PBS and dehydrated in graded ethanol (10%-100%) for 10 minutes each step. Finally, after critical point drying, the samples were mounted on stubs and were sputtered coated with gold.

NIH3T3 cell morphology was analyzed by light microscopy. NIH3T3 cells were suspended in 0.5 mL of supplemented DMEM and seeded in 24-well plates (10,000 cells/well). After incubation for 24 hours, the media were removed, and 100-extract from each composite was added. The culturing was stopped at days 2 and 5 of culture, and cell images were captured digitally (Eclipse TE2000-U microscope, Digital Sight DS-U1 camera, Nikon).

Cell adhesion assessment

NIH3T3 cells were seeded on the surface of the composites placed on 24-well plates at a density of 10,000 cells/well or on glass coverslips as controls, and then they were incubated in supplemented DMEM. NIH3T3 cell adhesion was observed using fluorescence microscopy through DAPI staining to determine the presence of nuclei. Cultures on all surfaces were stopped when the cells covered the entire glass coverslip. Then, they were washed several times with PBS, and cells were fixed with 4% paraformaldehyde solution, permeabilized with 0.1% Triton X-100 in PBS, and incubated with DAPI for 10 minutes at room temperature for each step. Subsequently, all samples were observed with a Nikon Eclipse TE2000-U microscope with a fluorescence filter (range 340-360 nm) for DAPI. The number of cells growing on composite surfaces was estimated using ImageJ software (n = 3 for each group).

The morphology of cells attached to the Ti-20HA surface was examined by SEM at 1 kV with variable magnification (×2,000 and ×5,000) (LAMARX-UNC). Cells adhered to the surface of composites were washed carefully with PBS and fixed overnight in 4% glutaraldehyde buffered in PBS at 4°C. Then, the samples were prepared as previously described.

Statistical analysis

Experimental data were expressed as means ± standard error of the mean (SEM). Results from the cytotoxicity and cell count were analyzed using 1-way ANOVA, and whenever the test indicated significant effects ($p<0.05$), a pairwise comparison (Newman-Keuls posttest) was also carried out. A p value <0.05 was considered to represent a significant difference in all cases.

Results

Surface characterization and in vitro bioactivity of the Ti-HA composites

The XRD pattern of the Ti-20HA composite showed characteristic peaks of Ti and HA (Fig. 1A). HA and Ti mainly existed in their simple substance, suggesting that reactions between HA and Ti did not take place. HA decomposition products were not identified. Peaks characteristic of titanium (near 2θ 40°) and a broad halo in the range 31°-34°, due to crystalline HA, were observed.

SEM micrographs of composite surfaces before immersion in SBF showed micropores and macropores on all surfaces, with HA particles well integrated into the Ti matrix (Fig. 1B, A). After 5 days of composite immersion, calcium phosphate deposition was observed (Fig. 1B, b), and at 10 days postimmersion, depositions covered the whole surface, especially into the pores (Fig. 1B, d). An energy-dispersive spectroscopy (EDS) spectrum is presented in Figure 1C.

Cytotoxicity

The cytotoxicity of the Ti-20HA as well as Ti and Ti-Por composites was evaluated in vitro by measuring Vero and NIH3T3 cell viability after incubation with the composite extracts for 24 hours. One-way ANOVA revealed a significant effect of 100-extracts of the different composites on Vero cell viability ($F_{(4,25)}$ =791.55, $p<0.0001$). Figure 2A shows that the percentages of viability for Ti-20HA (95.7% ± 0.81%; $p = 0.397$) and Ti (100.11% ± 1.35%; $p = 0.155$) were not significantly different from those of the negative control (98.50% ± 1.44%). Although viability of the cell exposed to Ti-Por 100-extract (88.83% ± 1.84%; $p<0.02$) was significantly lower than negative control, it was greater than 70%. According to the ISO 10993 standard, the samples are considered nontoxic whenever cell viability is greater than 70% (31). All groups ($p<0.001$) revealed percentages higher than that of the positive control (9.80% ± 0.83%).

In the same way, 1-way ANOVA showed a significant effect of 100-extracts of all composites on NIH3T3 cell viability ($F_{(4,25)}$=463.56, $p<0.0001$). The percentages of viability of NIH3T3 cells for the Ti-20HA, Ti and Ti-Por 100-extracts were 91.30% ± 2.38%, 92.30% ± 2.06% and 93.24% ± 1.64%, respectively, which were significantly different from the negative control group: 99.49% ± 1.52% ($p<0.02$) (Fig. 2B). Nevertheless, NIH3T3 viability was greater than 70% in all cases, thereby indicating a lack of extract composite toxicity to this cell line. Extract dilution did not show any effect on composite cytotoxicity (Fig. 2).

Cell morphological analysis

The Vero cell morphology did not reveal any differences between the cells incubated with supplemented DMEM medium or composite 100-extract (Fig. 3A, C, E). Moreover,

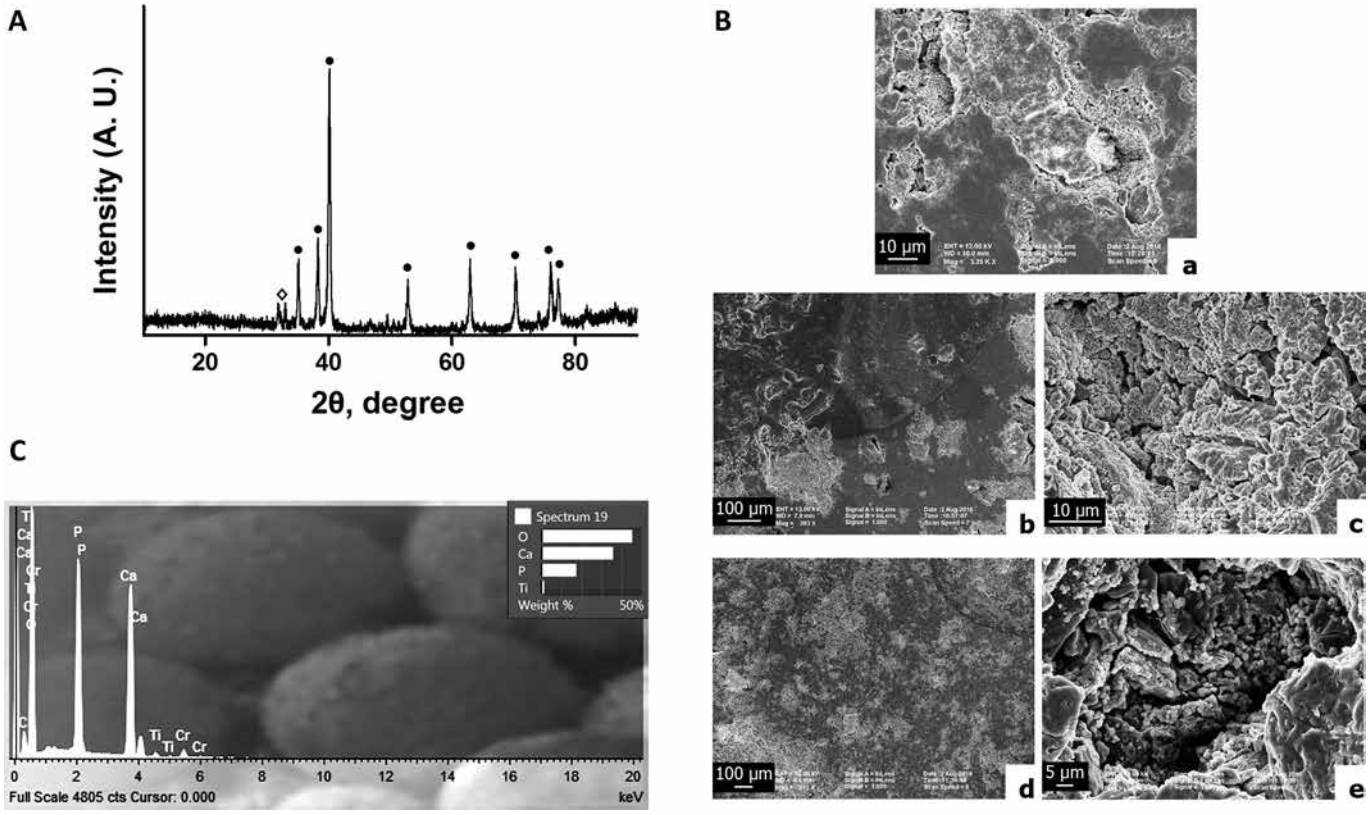

Fig. 1 - Characterization of Ti-HA composite surface. (**A**) X-ray diffraction of the Ti-HA composite. Ti (solid circles), HA (open diamond). (**B**) Scanning electron micrographs of composite. Composite surface before simulated body fluid (SBF) immersion (a). Composite surface after 5 days (b, c) and 10 days of SBF immersion (d, e). (**C**) Energy-dispersive spectroscopy (EDS) spectrum of the surface of Ti-20HA composite immersed in SBF for 10 days.

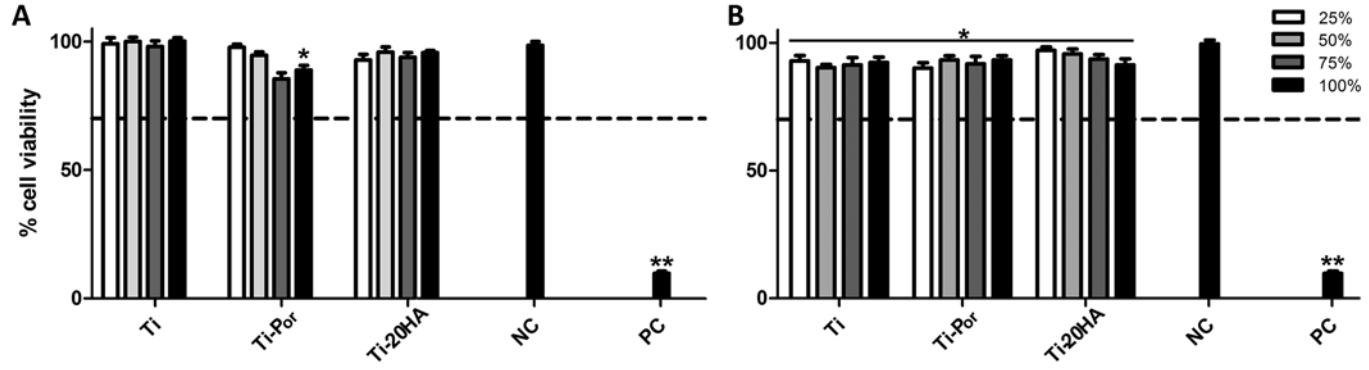

Fig. 2 - Cell viability for diluted extracts (25%, 50%, 75% and 100%) from Ti, porous Ti (Ti-Por) and Ti-20HA composites after cell culture for 24 hours,for Vero cells (**A**) and NIH3T3 cells (**B**). (N = 6). Values are means ± SEM. NC = negative control. *p<0.02, vs. NC; **p<0.001, vs. 100% extracts of different composites.

the cell confluence reached on day 4 of cell culture was similar among Ti-20HA, Ti-Por and control. In addition, composite extracts did not affect the cell size (Fig. 3B, D, F). Similar effects of different composite extracts on cell morphology, cell size and density of NIH3T3 lineage were also observed. After 2 and 5 days of incubation in the presence of extracts from Ti-20HA, Ti and Ti-Por, the microphotographs showed the NIH3T3 cells to be well attached and with similar morphologies compared with the controls (Fig. 4A-D). Furthermore, these cells proliferated widely between days 2 and 5 of incubation and were almost confluent on day 5 (Fig. 4E-H), indicating that the extracts did not alter their growth ability or development.

Cell adhesion

The micrographs showed that NIH3T3 cells stained with DAPI were able to attach to all surfaces (Fig. 5A), reaching

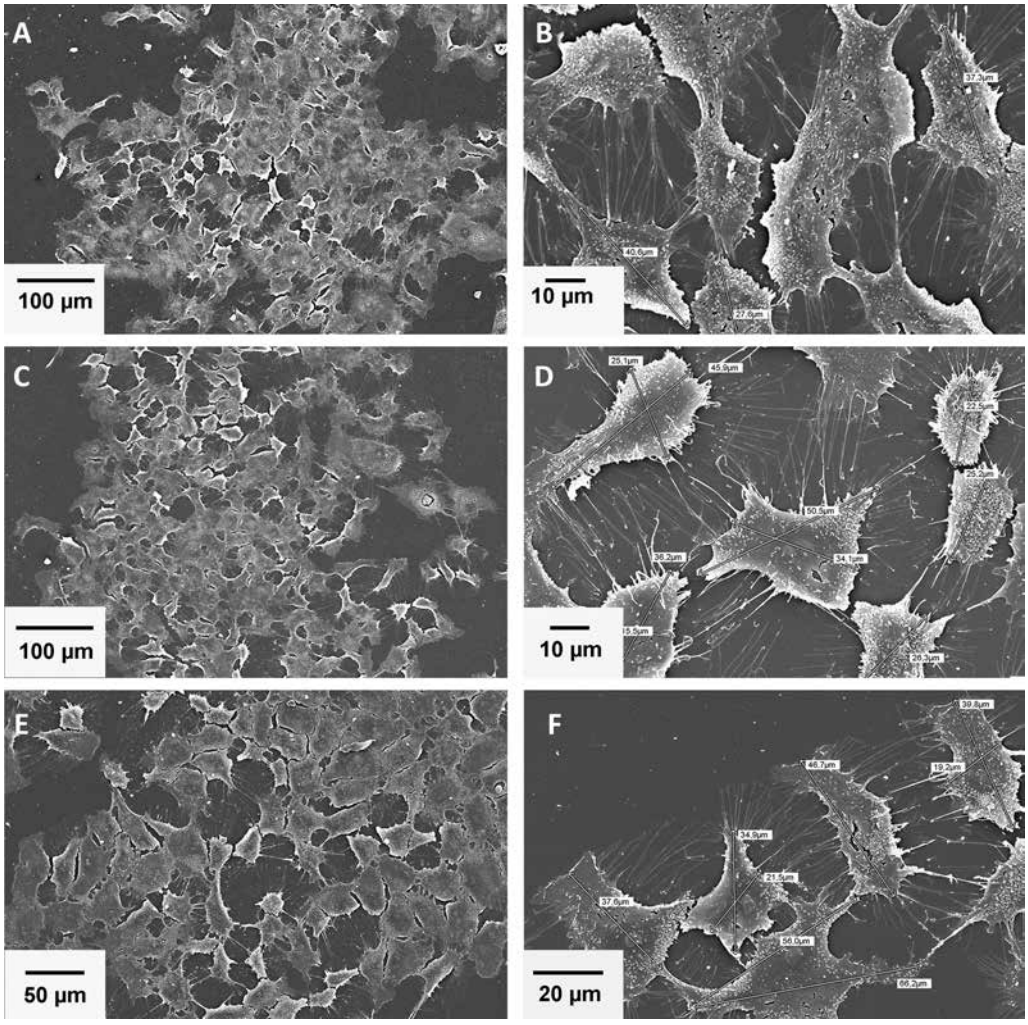

Fig. 3 - Scanning electron micrographs of Vero cells exposed for 24 hours to 100-extract of (**A, B**) Ti-HA, (**C, D**) porous Ti (Ti-Por), (**E, F**) supplemented DMEM (panels a,c: magnification ×200, bar = 100 µm; panel e: magnification ×300, bar = 50 µm; panels b,d: magnification ×1,000, bar = 10 µm; panel e: magnification ×900, bar = 20 µm).

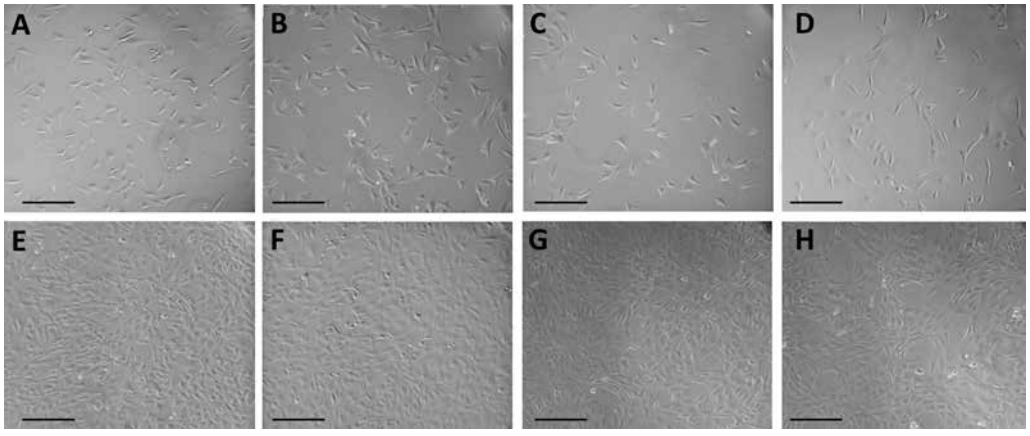

Fig. 4 - Representative phase contrast images of NIH3T3 cells cultured in 100-extracts of (**A**) supplemented DMEM, (**B**) Ti-20HA, (**C**) Ti and (**D**) porous Ti (Ti-Por) composites. Top panels: at day 2 of culture. Bottom panels: at day 5 of culture. Bars = 200 µm.

a similar density on surfaces of Ti-HA, Ti and Ti-Por (Fig. 5A b, d, f). Cell number was not significantly different between the 3 surfaces (Fig. 5B) ($p = 0.69$). These results suggest that Ti-20HA as well as Ti-Por and Ti composites were harmless to the cells. Furthermore, on the Ti-20HA surface, cells adhered to HA of the composite (Fig. 6B) and grew by spreading out across the surface with extensions observed of up to 10 µm in length (Fig. 6A, B). Cells also grew into the pores of the composite (Fig. 6C), thus supporting a possible biological fixation.

Discussion

In the present study we obtained a composite from Ti and bovine HA powders sintered at 800°C through the sim-

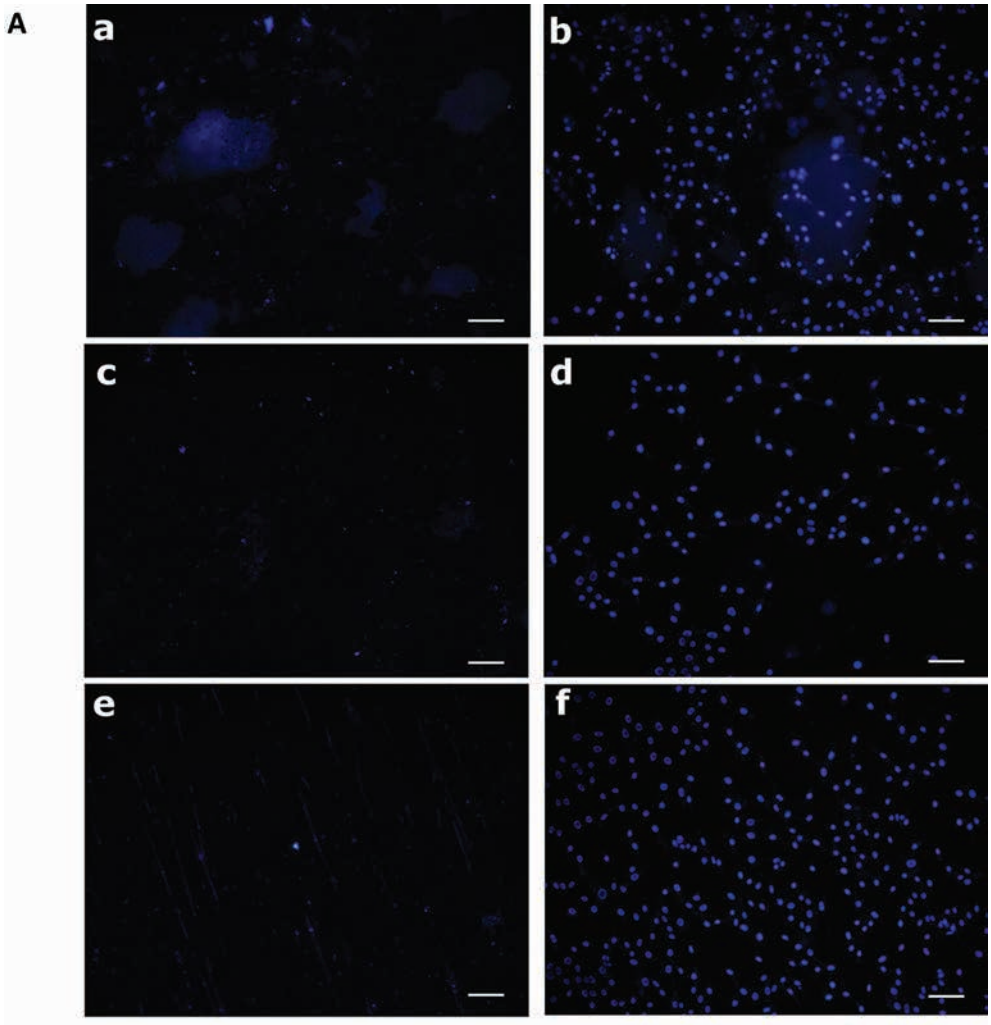

B

composite	Ti-20HA	Ti	Ti-Por
cell number/ field	487 ± 68	368 ± 95	417 ± 117

Fig. 5 - Representative fluorescence micrographs of NIH3T3 cell DAPI staining cultured for 96 hours on different composite surfaces. (**A**) cell grown on Ti-20HA (b); Ti (d) and Ti-Por (f) composites. Panels a, c, e: Ti-20HA, Ti and Ti-Por composites without cells. Bars = 100 µm. (**B**) Cell count by ImageJ software.

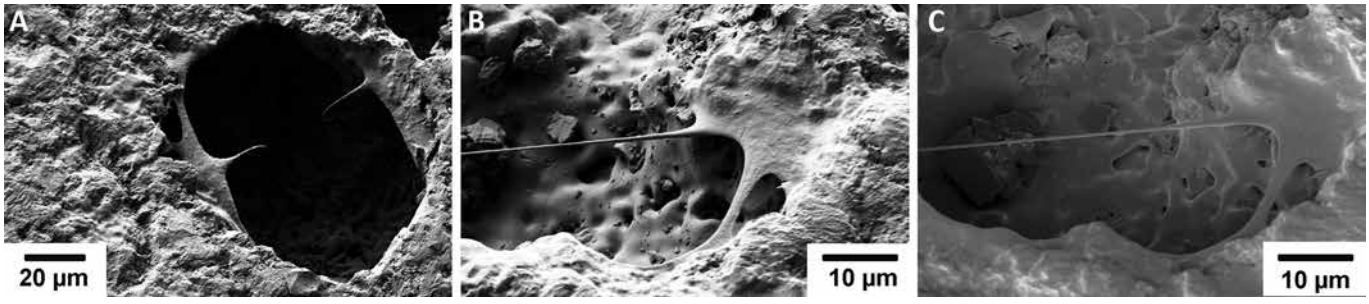

Fig. 6 - Scanning electron micrographs of NIH3T3 cells cultured for 96 hours on Ti-20HA surface (**A**): magnification ×2,000, bar = 20 µm; (**B**): magnification ×5,000, bar = 10 µm; (**C**): magnification ×5,000, bar = 10 µm).

ple and low-cost method of PM. The XRD pattern showed a composite with Ti and HA that mainly existed in their simple constituents. Micropores and macropores were observed on composite surfaces using SEM. After 10 days of immersion in SBF, the whole surface of the composite was covered with apatite, indicating its good bioactivity. Cytotoxicity assay did not reveal any toxicity of the composite to epithelial Vero or fibroblast NIH3T3 cells. Moreover, exposure of both these

cell types to composite extracts displayed similar morphologies to those grown in the presence of supplemented DMEM, thereby demonstrating the cytocompatibility of the extracts from the Ti-20HA composite sintered at 800°C. Additionally, NIH3T3 cells were able to proliferate and spread out on the Ti-20HA surface.

It is well known that HA is thermally stable up to 1250°C in air (35) and up to 1050°C in vacuum (36). However, in Ti-HA systems, it has been reported that the HA decomposition at temperatures above 800°C is related to the presence of Ti (27). For example, Ye et al (26) reported that Ti accelerated dehydroxylation of HA and stimulated the formation of tetracalcium phosphate and calcium oxide at temperatures below 1000°C. For this reason, we decided to work with a sintering temperature of 800°C to develop a stable composite, and we verified a good biological performance that to date had not been reported in the literature. Ti-HA composites have been developed by PM, which were sintered between 1000°C-1300°C (37) and demonstrated to be bioactive when immersed in SBF (23). Moreover, the cytocompatibility of Ti and Ti alloys have also been evaluated, and these showed different toxicity grades (38).

The capacity of apatite formation in SBF has been widely used to assess the bioactivity of biomaterials (30). Our results from SEM analysis showed that the composite was able to induce calcium phosphate deposition, covering the whole surface of the composite at 10 days post SBF immersion. Ning and Zhou (23) reported that calcium phosphate precipitations are bone-like apatite and would play an essential role in the formation of new bone (39).

On the other hand, cytotoxicity assay is one of the mandatory tests for biological safety evaluation of biomedical devices established in ISO 10993-5 (32). In this study, we used the MTT method to assess cytotoxicity, as an accurate indicator of potential toxicity in 2 cell lines. Figure 2 reveals cell viability higher than 70% for Vero and NIH3T3 cells when exposed to various diluted extracts from Ti, Ti-Por and Ti-20HA composites. This suggests that the Ti-20HA composite sintered at 800°C is not cytotoxic to either Vero or NIH3T3 cells, in accord with ISO 10993. Even more, the morphology and cell density of Vero and NIH3T3 cells cultured in 100-extract of Ti-20HA composites sintered at low temperature were similar to those cultured in supplemented DMEM (negative control). This assay showed a cell density and morphology preserved in both cell lines, indicating a high level of in vitro cytocompatibility for the Ti-20HA. It is accepted that the biomaterial in vitro compatibility is intimately related to cell behavior resulting from contact between cells and biomaterial – particularly to cell adhesion to their surfaces (40, 41). To investigate this, we evaluated NIH3T3 cells' ability to adhere to the Ti-20HA composite surface. The fluorescence images by DAPI staining in Figure 5 show NIH3T3 fibroblast cell adhesion on the Ti-20HA, indicating that cells were able to adhere to and proliferate on the composite surface by covering the whole surface at day 4 of culture. Additionally, SEM studies revealed contact among cells as well as the spreading of these on composite surface. Also, cells were even capable to grow into the pores on the Ti-20HA composite, establishing that there was good cytocompatibility of this composite. However, even if the ISO standard provides widely accepted parameters for proofs of biomaterials' cytocompatibility, it has some limitations, and these should be considered (42). Additional in vivo studies are still necessary to complete the evaluation of the composite, and to evidence its functionality, effectiveness, neovascularization, immune response and recellularization (43, 44).

These findings suggest that Ti-20HA composites sintered at low temperature are feasible to produce biological or bioactive fixation of the biomaterial, because the tissue was able to grow into the pores on the composite surface. This could be explained by the increased interfacial area between the tissue and the material, resulting in a higher inertial resistance to movement of the implant in the tissue (45). Therefore, surface porosity is considered to be one of the requirements for an ideal scaffold, because surface pores permit a successful diffusion of essential nutrients and oxygen for cell survival (46).

In summary, we have developed a new composite through a simple and low-cost method using PM with a promising biomedical application.

Disclosures

Financial support: This research was supported by grants from CONICET (PIP 112-201001-00495) and SECyT-Universidad Nacional de Cordoba (Argentina) (PIP 307-201101-00911CB).
Conflict of interest: The authors report no conflicts of interest.

References

1. Lowenstam HA, Weiner S. On biomineralization. 1st ed. Oxford, UK: Oxford University Press; 1989:88-305.
2. Weiner S, Wagner HD. Material bone structure-mechanical function relations. Annu Rev Mater Sci. 1998;28:1-658.
3. Dorozhkin SV; Dorozhkin SV. Calcium orthophosphates in nature, biology and medicine. Materials (Basel). 2009;2(2): 399-498.
4. Cao W, Hench LL. Bioactive materials. Ceram Int. 1996;22(6): 493-507.
5. Ong JL, Chan DC. Hydroxyapatite and their use as coatings in dental implants: a review. Crit Rev Biomed Eng. 2000;28(5-6): 667-707.
6. Shepherd JH, Shepherd DV, Best SM. Substituted hydroxyapatites for bone repair. J Mater Sci Mater Med. 2012;23(10)0: 2335-2347.
7. Kim HW, Li LH, Koh YH, Knowles JC, Kim H-E. Sol–gel preparation and properties of fluoride-substituted hydroxyapatite powders. J Am Ceram Soc. 2004;87(10):1939-1944.
8. Saranya K, Kowshik M, Ramanan SR. Synthesis of hydroxyapatite nanopowders by sol-gel emulsion technique. Bull Mater Sci. 2011;34(7):1749-1753.
9. Shepherd D, Best SM. Production of zinc substituted hydroxyapatite using various precipitation routes. Biomed Mater. 2013; 8(2):025003.
10. Akram M, Ahmed R, Shakir I, et al. Extracting hydroxyapatite and its precursors from natural resources. J Mater Sci. 2014; 49(4):1461-1475.
11. Jarcho M. Calcium phosphate ceramics as hard tissue prosthetics. Clin Orthop Relat Res. 1981;(157):259-278.
12. Gautier S, Champion E, Bernache-Assollant D, Chartier T. Rheological characteristics of aluminia platelet–hydroxyapatite composite suspension. J Eur Ceram Soc. 1999;19(4):469-477.
13. Nautiyal VP, Mittal A, Agarwal A, Pandey A. Tissue response to titanium implant using scanning electron microscope. Natl J Maxillofac Surg. 2013;4(1):7-12.

14. Polo-Corrales L, Latorre-Esteves M, Ramirez-Vick JE. Scaffold design for bone regeneration. J Nanosci Nanotechnol. 2014; 14(1):15-56.
15. Wang CK, Lin JH, Ju CP, Ong HC, Chang RP. Structural characterization of pulsed laser-deposited hydroxyapatite film on titanium substrate. Biomaterials. 1997;18(20):1331-1338.
16. Prosecká E, Buzgo M, Rampichová M, et al. Thin-layer hydroxyapatite deposition on a nanofiber surface stimulates mesenchymal stem cell proliferation and their differentiation into osteoblasts. J Biomed Biotechnol. 2012;2012:428503.
17. Roy M, Balla VK, Bandyopadhyay A, Bose S. Compositionally graded hydroxyapatite/tricalcium phosphate coating on Ti by laser and induction plasma. Acta Biomater. 2011;7(2): 866-873.
18. Hannora AE, Mukasyan AS, Mansurov ZA. Nanocrystalline hydroxyapatite/Si coating by mechanical alloying technique. Bioinorg Chem Appl. 2012;2012:390104.
19. Kim HW, Kim HE, Knowles JC. Fluor-hydroxyapatite sol–gel coating on titanium substrate for hard tissue implants. Biomaterials. 2004;25:3351-3358.
20. Eraković S, Janković A, Veljović D, et al. Corrosion stability and bioactivity in simulated body fluid of silver/hydroxyapatite and silver/hydroxyapatite/lignin coatings on titanium obtained by electrophoretic deposition. J Phys Chem B. 2013;117(6): 1633-1643.
21. Hayashi K, Inadome T, Mashima T, Sugioka Y. Comparison of bone-implant interface shear strength of solid hydroxyapatite and hydroxyapatite-coated titanium implants. J Biomed Mater Res. 1993;27(5):557-563.
22. Søballe K, Hansen ES, B-Rasmussen H, Jørgensen PH, Bünger C. Tissue ingrowth into titanium and hydroxyapatite-coated implants during stable and unstable mechanical conditions. J Orthop Res. 1992;10(2):285-299.
23. Ning C, Zhou Y. Correlations between the in vitro and in vivo bioactivity of the Ti/HA composites fabricated by a powder metallurgy method. Acta Biomater. 2008;4(6):1944-1952.
24. Karanjai M, Sundaresan R, Rao GV, Mohan TR, Kashyap BP. Development of titanium based biocomposite by powder metallurgy processing with in situ forming of Ca–P phases. Mater Sci Eng A. 2007;447(1-2):19-26.
25. Comín R, Reyna Musso LA, Cid MP, et al. Cytotoxicidad de Hidroxiapatita y su morfología en composites con Ti. Lat Am Trans IEEE. 2013;11(1):103-106.
26. Ye H, Liu XY, Hong H. Characterization of sintered titanium/hydroxyapatite biocomposite using FTIR spectroscopy. J Mater Sci Mater Med. 2009;20(4):843-850.
27. Weng I, Liu X, Zhang X, Ji X. Thermal decomposition of hydroxyapatite structure induced by titanium and its dioxide. J Mater Sci Lett. 1994;13(3):159-161.
28. Popa C, Simon V, Vida-Simiti I, Batin G, Candea V, Simon S. Titaniumhydroxyapatite porous structures for endosseous applications. J Mater Sci Mater Med. 2005;16(12):1165-1171.
29. International Organization for Standardization. Biological evaluation of medical devices. ISO 10993. Part 1: Evaluation and testing in the risk management process. Geneva, Switzerland: International Organization for Standardization; 2009.
30. Kokubo T, Takadama H. How useful is SBF in predicting in vivo bone bioactivity? Biomaterials. 2006;27(15):2907-2915.
31. International Organization for Standardization. Biological evaluation of medical devices. ISO 10993. Part 12: Sample preparation and reference materials. Geneva, Switzerland: International Organization for Standardization; 2012.
32. International Organization for Standardization. Biological evaluation of medical devices. ISO 10993. Part 5: Tests for in vitro cytotoxicity. Geneva, Switzerland: International Organization for Standardization; 2009.
33. Mosmann T. Rapid colorimetric assay for cellular growth and survival: application to proliferation and cytotoxicity assays. J Immunol Methods. 1983;65(1-2):55-63.
34. Modglin VC, Brown RF, Jung SB, Day DE. Cytotoxicity assessment of modified bioactive glasses with MLO-A5 osteogenic cells in vitro. J Mater Sci Mater Med. 2013;24(5):1191-1199.
35. Weng J, Liu X, Zhang X, Ma Z, Ji X, Zyman Z. Further studies on the plasma-sprayed amorphous phase in hydroxyapatite coatings and its deamorphization. Biomaterials. 1993;14(8):578-582.
36. Trombe JC, Montel G. Some features of the incorporation of oxygen in different oxidation states in the apatitic lattice: Part III: synthesis and properties of some oxygenated apatites. J Inorg Nucl Chem. 1978;40(1):27-30.
37. Salman S, Gunduz O, Yilmaz S, et al. Sintering effect on mechanical properties of composites of natural hydroxyapatites and titanium. Ceram Int. 2009;35(7):2965-2971.
38. Song YH, Kim MK, Park EJ, Song HJ, Anusavice KJ, Park YJ. Cytotoxicity of alloying elements and experimental titanium alloys by WST-1 and agar overlay tests. Dent Mater. 2014;30(9): 977-983.
39. Tanigawa H, Asoh H, Ohno T, et al. Electrochemical corrosion and bioactivity of titanium–hydroxyapatite composites prepared by spark plasma sintering. Corros Sci. 2013;70: 212-220.
40. Valerio P, Oktar FN, Goller G, et al. Evaluation of osteoblasts viability, alkaline phosphatase production and collagen secretion in the presence of TiHA. Key Engineering Materials. 2004; 254-256;777-780.
41. Varoni E, Canciani E, Palazzo B, et al. Effect of poly-L-lysine coating on titanium osseointegration: from characterization to in vivo studies. J Oral Implantol. 2015;41(6):626-631.
42. Bruinink A, Luginbuehl R. Evaluation of biocompatibility using in vitro methods: interpretation and limitations. Adv Biochem Eng Biotechnol. 2012;126:117-152.
43. Sampaio BV, Goller G, Oktar FN, Valério P, Goes A, Leite MF. Biocompatibility evaluation of three different titanium-hydroxyapatite composites. Key Eng Mater. 2005;284-286:639-642.
44. Harrasser N, de Wild M, Gorkotte J, et al. Evaluation of calcium dihydroxide- and silver-coated implants in the rat tibia. J Appl Biomater Funct Mater. 2016;14(4):e441-e448.
45. Narayanan R, Seshadri SK, Kwon TY, Kim KH. Calcium phosphate-based coatings on titanium and its alloys. J Biomed Mater Res B Appl Biomater. 2008;85(1):279-299.
46. Bose S, Roy M, Bandyopadhyay A. Recent advances in bone tissue engineering scaffolds. Trends Biotechnol. 2012;30(10): 546-554.